JOURNAL OF CATALYSIS 74, 110–120 (1982)

Ammonia Synthesis on Osmium Powder and Hydrogenation of Preadsorbed Nitrogen from 100 to 500°C

GÉRARD RAMBEAU, AHMED JORTI, AND HENRI AMARIGLIO

Laboratoire Maurice Letort, CNRS, Route de Vandoeuvre, Boîte Postale No. 104, 54600 Villers Nancy, France, and Université de Nancy I, Boulevard des Aiguillettes, 54037 Nancy Cédex, France

Received July 20, 1981

The kinetic analysis of NH_3 synthesis over powdered Os shows that the rate law is $r = kP_{N_2} \cdot P_{H_2}^{-1} \cdot (1 + KP_{NH_3})^{-2}$. The reaction is therefore limited by N_2 adsorption and inhibited by H_2. It is also inhibited by NH_3 but at a lesser level. The high rate of hydrogenation of preadsorbed N_2 down to 100°C exemplifies the rate limitation by N_2 adsorption. The latter can hardly be detected below 200°C. Hydrogenation of preadsorbed nitrogen makes it possible to know the amount of nitrogen adsorbed for a given time so that the rate of adsorption can be reached. That rate represents the intrinsic catalytic activity of Os which turns out to be about 100 times higher than that of Fe but 100 times lower than that of Ru, at 200°C. At about 400°C and if the activities are referred to the stoichiometric reactant mixture, Fe is a little more active than Ru and 100 times more active than Os.

1. INTRODUCTION

We have confirmed previously (*1*) that the rate of NH_3 synthesis on Fe can be expressed as $r = kP_{N_2}(1 + KP_{NH_3})^{-2}$. This rate law reveals a rate limitation of the reaction by N_2 chemisorption and an inhibition by NH_3. On powdered Ru (*2*), N_2 adsorption is the rate-limiting step again since $r = kP_{N_2} \cdot P_{H_2}^{-1}$; however, there is no longer inhibition by NH_3 but instead a strong inhibition by H_2 appears. On Ru the rate of adsorption of N_2 can be several orders of magnitude higher than the rate of synthesis provided that the catalyst is exposed to *pure* N_2. As the hydrogenation of the preadsorbed nitrogen is fast, a process has been derived according to which NH_3 can be produced by alternate exposures of the catalyst to N_2 and H_2. Greater advantage is thus taken of the high potential activity of Ru (*3*) since a great part of that activity does not appear under usual permanent conditions due to the H_2 inhibition. With the appropriate cyclic procedure, Ru becomes a better catalyst than Fe and might allow performances to be reached comparable with industrial ones but at atmospheric pressure.

It therefore became interesting to look for the behavior of the third metal of the same column in the Periodic Table. As will now be reported the properties of Os display similarities to those of both Ru and Fe.

As in the case of Ru, comparison with literature data is difficult. Not only has Os been little examined but it has most often been used in a supported form and promoted with alkali metals. In addition it has been studied under steady conditions and with reference to compositions of the reactant mixture very close to the stoichiometric one (*4–7*).

2. EXPERIMENTAL

2.1. Kinetic Measurements

The experiments are performed at atmospheric pressure in a flow-type apparatus which has already been described (*2*).

The reactor may be fed with N_2, H_2, He, or any mixture of these gases after careful purification through Cu filings at 250°C and a trap filled with glass beads at liquid air

0021-9517/82/030110-11$02.00/0

temperature. The exit gas bubbles through a sulphuric acid solution (10^{-2}, 10^{-3}, or 10^{-4} *N*) and the progressive neutralization of H_2SO_4 by the ammonia produced is detected by a conductimetric cell.

The steady rate of production of NH_3, R_s, is determined by measuring the time required to neutralize a known and appropriate sample of acid solution (5 to 50 cm^3). The rate can thus be known within ±1% down to 10^{-8} mole min^{-1}.

The flow rates of gases are measured by using a soap-bubble flowmeter at the exit of the apparatus. From R_s and the flow rate of reactant mixture, F, the effluent partial pressure of NH_3, P_s, can be derived as $P_s = R_s \cdot RT/F$.

The amount of N_2 adsorbed on Os during an exposure of the metal to that gas can also be measured by substituting H_2 for N_2 and measuring the resulting amount of NH_3. The ammonia produced neutralizes some fraction of the sample of acid solution and the amount of acid reacted is derived from the variation of the conductivity.

2.2. *Catalyst*

The catalyst is 1 g of very pure Os powder (Johnson & Matthey, Specpure sponge, 10 ppm total impurity). Its active area is determined as reported later.

The powder is first reduced under a flow of reactant mixture ($N_2 + 3H_2$) while its temperature is progressively increased up to 500°C.

3. RESULTS

When the reaction conditions are changed, the catalyst response is slower than in the case of Ru but it is always accounted for by a mere adjustment of the composition of the chemisorbed film. No surface modification appears therefore as was the case with Fe (*8, 9*). Thereafter, Os activity is very stable and it is easy to study the influence of kinetic factors upon it.

3.1. *Inhibition by NH_3*

In order to examine the effect of NH_3 pressure on the rate of reaction, the flow rate of the reactant mixture must be changed while maintaining its composition constant. Curve 1 of Fig. 1 shows how little is the influence of the flow rate upon the rate of production of NH_3 at 401°C and for a nearly stoichiometric mixture. As will be shown in the Discussion, if R_s depends on P_{NH_3}, the rate R_0 corresponding to $P_{NH_3} = 0$ can be computed from the equation

$$R_0 = R_s\left(1 + mP_s + \frac{m^2P_s^2}{3}\right), \qquad (1)$$

where P_s stands for P_{NH_3} at the reactor outlet and where m is a parameter which depends upon P_{H_2} but not upon P_{N_2}. Only two

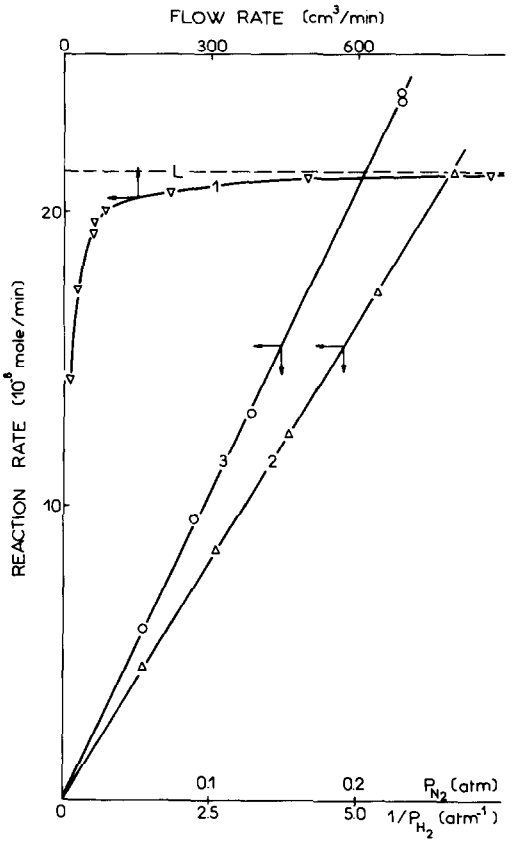

FIG. 1. Curve 1: reaction rate as a function of flow rate (27% N_2–73% H_2; 401°C). Curve 2: reaction rate as a function of N_2 pressure (P_{H_2} = 0.73 atm; 401°C). Curve 3: reaction rate as a function of $1/P_{H_2}$ (P_{N_2} = 0.26 atm; 370°C). Level L: reaction rate at $P_{NH_3} = 0$ (27% N_2–73% H_2; 401°C).

sets of values for R_s and P_s, at every temperature, allow one to calculate R_0 and m and to obtain the complete variation of R_s as a function of P_s as well.

Curve 1 of Fig. 2 illustrates the results of such a calculation starting from the data of curve 1 of Fig. 1. As the variation is linear one deduces that $m^2P_s^2/3 \ll 1$ so that

$$R_s = R_0 - mR_0P_s.$$

The intercept with the rate axis gives R_0 and m is then derived from the slope. R_0 represents the level L towards which the rate R_s tends in Fig. 1 when the flow rate increases. We can conclude that our maximum flow rate (1000 cm³/min) is sufficient to reach R_0 directly within a good approximation ($mP_s = 5 \times 10^{-3} \ll 1$).

3.2. Kinetic Orders

P_{N_2} is easily varied by substitution of He for a variable part of N_2 in the reactant mixture. The total pressure (1 atm) and P_{H_2} (0.73 atm) are kept constant. The flow rate is maintained at its maximum value (1000 cm³/min). The decrease of P_{N_2} results in a similar decrease of P_s and mP_s as m remains constant. The inhibition by NH_3 becomes more and more negligible so that R_s remains nearly equal to R_0. The straight line 2 in Fig. 1 shows the variation of R_0 as a function of P_{N_2} at 401°C. Therefore, the reaction order with respect to N_2 is 1 as is the case on Fe and Ru.

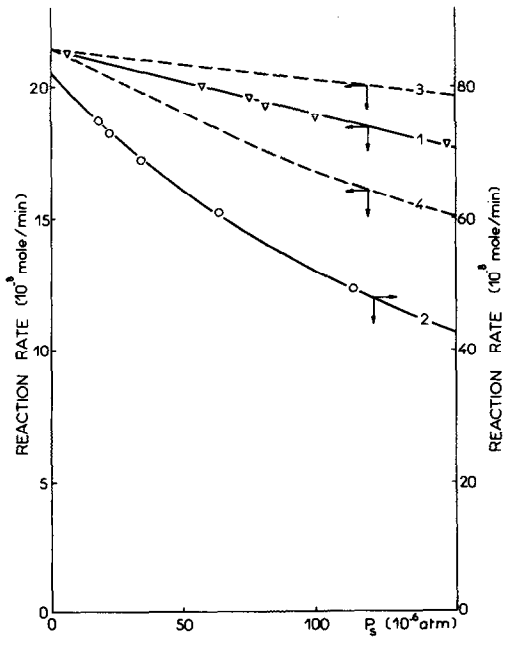

FIG. 2. Reaction rate versus effluent ammonia partial pressure at 401°C. Curve 1: $P_{N_2} = 0.27$ atm; $P_{H_2} = 0.73$ atm; $m = 1.1 \pm 0.05 \times 10^3$ atm^{-1}. Curve 2: $P_{N_2} = 0.25$ atm; $P_{H_2} = 0.17$ atm; $m = 4.75 \pm 0.25 \times 10^3$ atm^{-1}. Curve 3: 27% N_2–73% H_2; $m = 0.55 \times 10^3$ atm^{-1}. Curve 4: 27% N_2–73% H_2; $m = 2.3 \times 10^3$ atm^{-1}.

Determining the reaction order with respect to H_2 is less easy. Any decrease of P_{H_2}, with F and P_{N_2} kept constant, results in increasing values of P_s and m as well, and the inhibition by NH_3 increases. Curve 2 of Fig. 2 shows that the variation of R_s as a function of P_s is no longer linear for a H_2 content equal to 17%. Equation (1) cannot be applied in its approximate form to calculate m and R_0. Both quantities appear proportional to $P_{H_2}^{-1}$ (curves 1 and 2 of Fig. 2). It will be shown in the Discussion that the proportionality of m to $P_{H_2}^{-1}$ reveals that NH_2 is the most abundant species on the surface at 400°C. The -1 order of the reaction rate with respect to P_{H_2} is still more obvious at 370°C (straight line 3, Fig. 1) and reveals a strong H_2 inhibition.

3.3. Arrhenius Plots

Figure 3 illustrates the rate variations as a function of temperature. Curves 1 and 1′ relate to two different values of the flow rate for the nearly stoichiometric mixture. One can see that the contact time of the reactant mixture has but little influence except for the equilibrium region (the equilibrium is reached along the rising linear part of curve 1′). One can conclude that the inhibition by NH_3 is not sufficient to separate the decreasing (or truly kinetic) linear parts of curves 1 and 1′ which give therefore the rate R_0 against $1/T$ down to about 330°C. This is not the case in curve 2 which relates to a mixture containing 17% H_2 and for which the inhibition by NH_3 is notice-

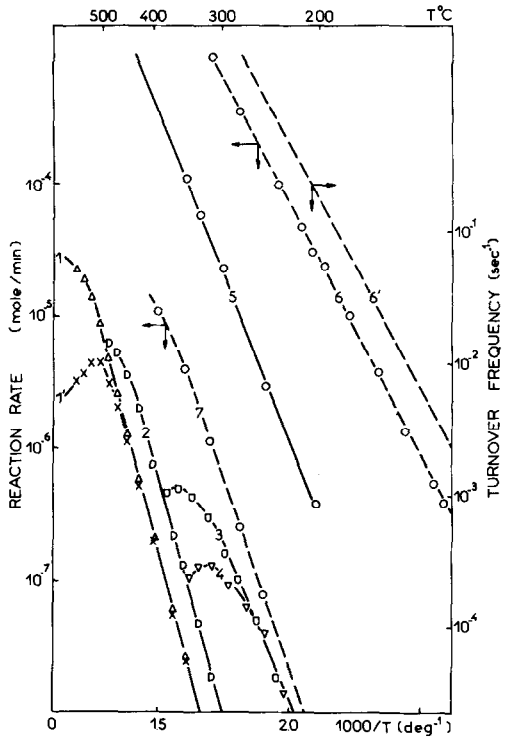

FIG. 3. Reaction rate as a function of $1/T$. Curves 1 and 1': 1000 and 100 cm^3/min; 27% N_2–73% H_2. Curve 2: 1000 cm^3/min; 25% N_2–17% H_2–He. Curves 3 and 4: 1000 cm^3/min; N_2 + 0.8% H_2 and 0.2% H_2. Curve 5: rate of adsorption of N_2 at zero coverage of the surface (P_{N_2} = 0.27 atm). Curves 6 and 6': the same as curve 5 for 1 g of Ru. Curve 7: the same as curve 5 for 1 g of Fe.

able at about 400°C even for the highest value of the flow rate (curve 2, Fig. 2). This inhibition decreases as a function of the temperature since the order −1 with respect to H_2 can be observed directly on R_s at about 300°C (comparison of curves 1 and 2, Fig. 3).

As in the case of Ru (*2*), an appreciable lowering of the lowest temperature of NH_3 detection is expected from a strong decrease of the H_2 content of the reactant mixture. This is observed in curve 3 (Fig. 3) corresponding to 0.8% H_2 in 1000 cm^3/min of N_2 as the NH_3 production can be monitored down to 230°C. At higher temperatures, high rates of production cannot be reached because the decrease of the H_2 pressure causes the equilibrium to shift towards lower NH_3 pressures. If H_2 pressure is decreased still more (curve 4, 0.2%) no more increase of activity at low temperatures can result but a new decrease of the equilibrium NH_3 content is evidenced. The common parts of curves 3 and 4 give the highest activities that can be obtained at low temperatures as decreasing again the H_2 content causes a lowering of the rate at every temperature and leads to a curve which would be completely under curve 4.

3.4. Adsorption of N_2 in the absence of H_2

In order to study the adsorption of N_2 on Os, the catalyst is flushed with pure N_2 for a given time and thereafter with pure H_2. The flow rate of both gases is sufficient (750 cm^3/min) for the catalyst bed to be cleared quickly (5×10^{-2} sec). A short flow of helium separates the two gases to prevent them from diffusing into one another. The amount of NH_3 which is produced when the catalyst is submitted to H_2 gives that of N_2 which was adsorbed.

Curve 1 of Fig. 4 represents the way according to which the amount of N_2 adsorbed at 202°C increases as a function of the time of adsorption. An inflexion point is observed as in the case of Ru (*2*). The unexpected increase of the rate of adsorption at the beginning of the exposure to N_2 is explained as previously by the fact that the metal surface is completed with H_2 initially. To check this point the catalyst is flushed with He after the hydrogenation period (until total desorption of H_2) and before the feed with N_2. Curve 2 results with the expected decrease of adsorption rate from the beginning.

The inflexion point can still be observed at 252°C (curve 3) but not at temperatures higher than 300°C (curves 4, 5, 6) due to the corresponding high rate of H_2 desorption.

The maximum amount of N_2 adsorbed is the same from 200 to 300°C and is reached within a few minutes or tens of minutes

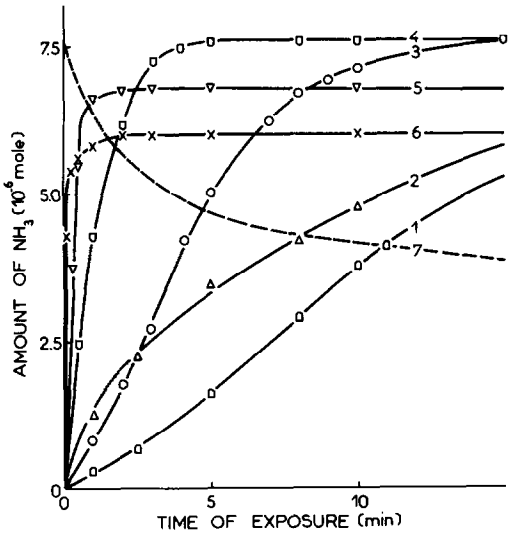

FIG. 4. Amounts of NH_3 resulting from hydrogenation of preadsorbed N_2 as a function of the length of the flush by N_2 at 202°C (hydrogenated catalyst: (1); dehydrogenated catalyst: (2)), 252°C (3), 300°C (4), 350°C (5), and 399°C (6). Influence of the length of the flush by He on the residual amount of preadsorbed N_2 at 300°C (7).

depending on the temperature. As for Ru, the surface of Os can be saturated with N_2.

N_2 desorption can be observed too if the catalyst is flushed for a given time with He before being submitted to H_2 and after saturation with N_2. Curve 7 (Fig. 4) shows the result of such a procedure at 300°C. As the desorption process occurs at a measurable rate, the maximum amount of N_2 adsorbed corresponds to the establishment of the adsorption–desorption equilibrium. The resulting decrease of this amount as a function of temperature is seen in curves 4, 5, and 6. However, the adsorption process is irreversible at 200°C since no N_2 desorption can be observed at this temperature even after a flow of about 10 h with He.

3.5. *Active Area*

Our determination of the amount of N_2 corresponding to the saturation of the surface is a way to know the quantity of sites which are able to adsorb N_2 and allow it to react into NH_3. We can therefore state that the amount of sites which are able to catalyze the reaction under steady conditions is $L = 7.5 \times 10^{-6}$ mole of sites/g. The reaction rates given in Fig. 3 can thus be converted into turnover frequencies.

The knowledge of L gives a way to determine the nitrogen surface coverage, θ_N, in N_2 adsorption experiments. We have shown previously (*2*) that

$$\frac{\theta_N}{1 - \theta_N} = \frac{r_0}{L} t,$$

where r_0 stands for the rate of adsorption on a *bare* surface and t for the time of adsorption on the dehydrogenated catalyst.

Figure 5 shows the variation of $\theta_N/(1 -$

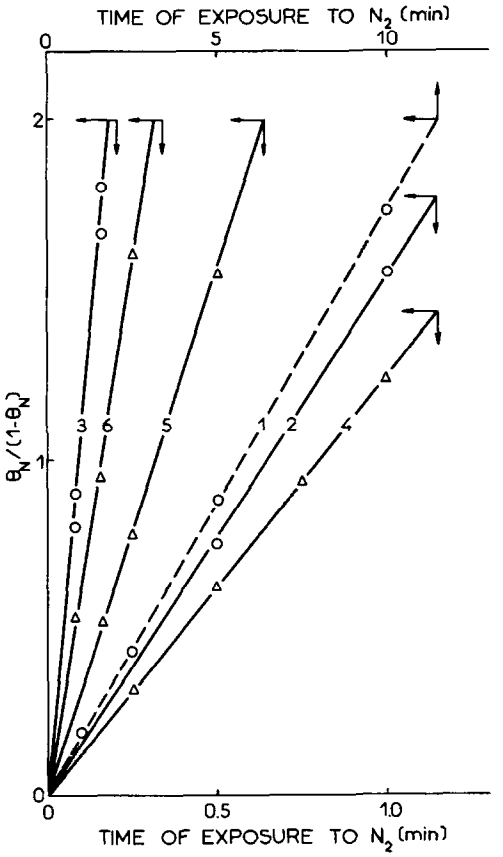

FIG. 5. $\theta_N/(1 - \theta_N)$ plotted against the length of the flush by N_2 of the initially dehydrogenated catalyst under $P_{N_2} = 1$ atm at 202°C (1), 252°C (2), and 302°C (3) or under $P_{N_2} = 0.11$ atm at 302°C (4), 326°C (5), and 352°C (6).

θ_N) as a function of t at different temperatures. The slopes of curves 1, 2, and 3, once multiplied by L, give r_0 corresponding to P_{N_2} = 1 atm at 202, 252, and 302°C. At 300°C the adsorption is too fast under 1 atm and N_2 is diluted into He. The straight lines 4, 5, and 6 result at 302, 326, and 352°C for P_{N_2} = 0.11 atm. The comparison of the slopes of curves 3 and 4 makes it possible to show that the rate of adsorption is proportional to P_{N_2}. We can thus calculate the rate of adsorption of N_2 under 0.27 atm at different temperatures and plot its variation against $1/T$ (curve 5, Fig. 3).

3.6. *Hydrogenation of N_2 Preadsorbed*

Figure 6 shows the amount of NH_3 which is produced when the sample, first saturated with N_2, is flushed with pure H_2 as a function of the time of hydrogenation. Half the monolayer of nitrogen is extracted within less than 0.1 min at 300 to 200°C.

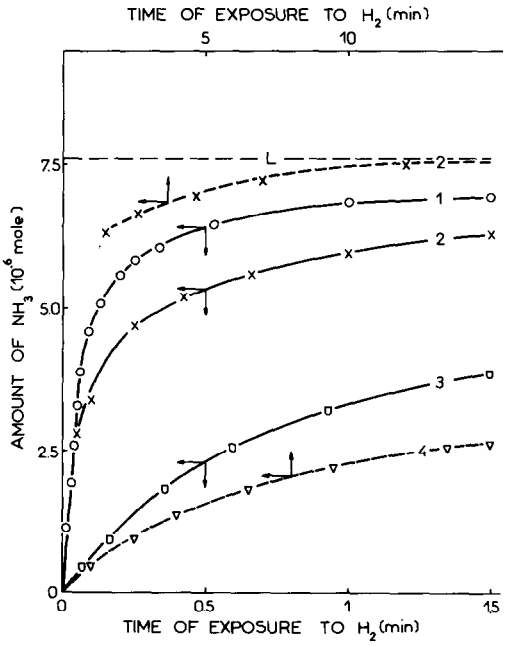

FIG. 6. Amounts of NH_3 resulting from hydrogenation of the surface saturated with N_2 as a function of the time on stream under H_2 at 301°C (1), 203°C (2), 153°C (3), and 100°C (4); P_{H_2} = 1 atm; 700 cm³/min. L: total amount of active sites.

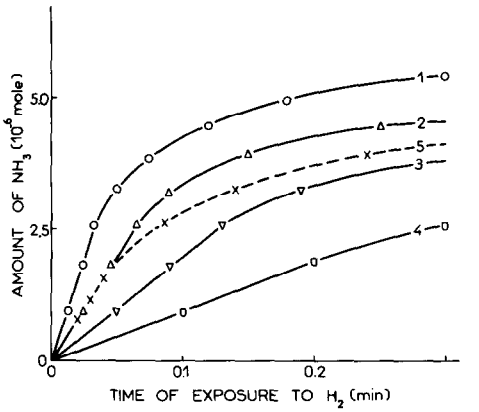

FIG. 7. Amounts of NH_3 resulting from hydrogenation of the surface saturated with N_2 at 301°C as a function of the time on stream under H_2 at the flow rate of 700 cm³/min (P_{H_2} = 1 atm: (1); P_{H_2} = 0.25 atm: (5)), 350 cm³/min (2), 175 cm³/min (3), and 87 cm³/min (4).

The hydrogenation process slows down at 150°C (curve 3) and becomes difficult at 100°C (curve 4). It can no longer be detected at room temperature, in strong contrast with Ru upon which the production of NH_3 can be detected down to −70°C. The hydrogenation runs carried out at temperatures lower than 200°C have been preceded by N_2 adsorption and 200°C as it would have been too slow at the temperature of the experiment.

In Fig. 7 the beginning of the hydrogenation process is developed at different values of the H_2 flow rate. One can see that the amount of NH_3 produced is proportional to the time at the start of the process. By comparison of the initial slopes of the curves we can deduce that the amount of NH_3 which is produced within a given time is proportional to the flow rate. The NH_3 pressure is therefore constant at the outlet of the reactor when the time of hydrogenation and the flow rate are varied at the beginning of the hydrogenation process. This clearly means that an overall equilibrium operates between H_2 and NH_3 in the gas phase and adsorbed N_2. The NH_3 pressure remains constant inasmuch as the end of the catalyst remains completely covered with N_2 and this is the case initially until

consumption of one-third of the monolayer of N_2.

From the coincidence of the initial parts of curves 2 (350 cm³/min; 100% H_2) and 5 (700 cm³/min; 25% H_2) we conclude that the equilibrium pressure of NH_3 is proportional to $P_{H_2}^{1/2}$. We shall see in the Discussion that this kind of influence of P_{H_2} reveals that the most abundant species on the surface is adsorbed NH_3 at 300°C.

4. DISCUSSION

4.1. Rate Law and Mechanistic Inferences

As on Fe (*1*, *10*) and Ru (*2*, *11*) the rate limitation by N_2 adsorption can be inferred from the first order of the reaction rate with respect to N_2. This conclusion is borne out by the equilibrium being readily attained when preadsorbed N_2 is reacted with H_2, as for Fe (*12*) and Ru (*3*). The hydrogenation of preadsorbed N_2 can proceed even at temperatures which would be too low for allowing N_2 to adsorb on the metal. The possibility of a molecular adsorption of N_2 can be discarded as it was on Ru (*2*) due to the kinetic order of -1 with respect to H_2. The usual mechanism can therefore be considered:

$$\begin{aligned}
&S\text{–}S + N_2 \rightarrow 2SN,\\
&S\text{–}S + H_2 = 2SH,\\
&SN + SH = SNH + S,\\
&SNH + SH = SNH_2 + S,\\
&SNH_2 + SH = SNH_3 + S,\\
&SNH_3 = S + NH_3.
\end{aligned}$$

The adsorption equilibrium of H_2 can be expressed as

$$(SH)/(S) = (KP_{H_2})^{1/2},$$

whereas the equilibrium between H_2 and NH_3 in the gase phase and every NH_x surface species leads to

$$P_{NH_3} = K_{NH_3}\frac{(SNH_3)}{(S)} = K_{NH_2}P_{H_2}^{1/2}\frac{(SNH_2)}{(S)} = K_{NH}P_{H_2}\frac{(SNH)}{(S)} = K_N P_{H_2}^{3/2}\frac{(SN)}{(S)}.$$

The total number of active sites, either bare or covered, which are present on the sample surface is given by

$$L = (S)\left[1 + (KP_{H_2})^{1/2} + \left(\frac{1}{K_N P_{H_2}^{3/2}} + \frac{1}{K_{NH}P_{H_2}} + \frac{1}{K_{NH_2}P_{H_2}^{1/2}} + \frac{1}{K_{NH_3}}\right)\cdot P_{NH_3}\right].$$

The steady rate of reaction expressed in mole of NH_3 per minute per gram is equal to that of N_2 adsorption (*2*)

$$r = 2k(S\text{–}S)P_{N_2} = kLP_{N_2}(S)^2/L^2$$

and finally

$$r = \frac{kLP_{N_2}}{[1 + (KP_{H_2})^{1/2}]^2\,(1 + mP_{NH_3})^2}$$

with

$$m = \left(\frac{1}{K_N P_{H_2}^{3/2}} + \frac{1}{K_{NH}P_{H_2}} + \frac{1}{K_{NH_2}P_{H_2}^{1/2}} + \frac{1}{K_{NH_3}}\right)[1 + (KP_{H_2})^{1/2}]^{-1}. \quad (2)$$

It results that

$$mP_{NH_3} = \frac{(SN) + (SNH) + (SNH_2) + (SNH_3)}{(S) + (SH)}. \quad (3)$$

The preceding rate law assumes that the adsorption of N_2 is irreversible and this is valid on condition that $k(S)^2 P_{N_2} \ll k'(SN)^2$ and therefore $(P_{NH_3}/P_e)^2 \ll 1$, where k' is the rate constant of the N_2 desorption and where P_e is the pressure of NH_3 at equilibrium. All of the data of Figs. 1 and 2 meet this requirement.

In curve 1 of Fig. 1 the rate ends by becoming independent of the flow rate when the latter is high enough for mP_{NH_3} to be much less than 1. It follows that the rate of production can be written as

$$R_s = R_0 = \frac{kLP_{N_2}}{[1 + (KP_{H_2})^{1/2}]^2} = \frac{r_0}{[1 + (KP_{H_2})^{1/2}]^2} \quad (4)$$

as r_0 is the rate of N_2 adsorption on the bare surface. In such a case Os behaves exactly as the powder of Ru (*2*) on which no inhibition by NH_3 occurs. On the contrary in the case illustrated by curve 2 of Fig. 2 the inhibition by NH_3 does not disappear even at high flow rates. Os behaves then as Fe (*1*) and R_0 has to be calculated. As the extent of reaction is small ($P_s/P_e \leq 10^{-1}$, $P_e \leq 10^{-3}$ atm) P_{N_2}, P_{H_2}, and the flow rate F may be assumed constant.

If the differential mass-balance equation

$$\frac{F}{RT}\,dP_{NH_3} = \frac{kP_{N_2}dL}{[1 + (KP_{H_2})^{1/2}]^2(1 + mP_{NH_3})^2}$$

is integrated between the inlet ($P_{NH_3} = 0$) and the outlet ($P_{NH_3} = P_s$) of the catalyst bed, Eq. (1) used in the experimental work is derived.

Our calculation assumes that the reactor is of the plug-flow type. However, this assumption is not too severe inasmuch as a stirred-flow reactor would lead to

$$R_s = \frac{R_0}{(1 + mP_s)^2} = \frac{R_0}{1 + m'P_s + m'^2P_s^2/4}$$

with $m' = 2m$. This equation differs from (1) by the square term only. The difference between both square terms remains negligible under our experimental conditions. Both equations result in the same value of R_0 within a good approximation.

Obviously Eq. (4) accounts for the first order with respect to N_2. The order with respect to H_2 (-1) is also accounted for on condition that

$$(KP_{H_2})^{1/2} = \frac{(SH)}{(S)} \gg 1. \qquad (5)$$

On the other hand, m is inversely proportional to P_{H_2} at 400°C (Fig. 2, curves 1 and 2). If Eqs. (2), (3), and (5) are referred to, this behavior can be displayed on the condition that

$$m = \frac{1}{K_{NH_2}K^{1/2}P_{H_2}},$$

that is to say $$mP_{NH_3} = \frac{(SNH_2)}{(SH)} \qquad (6)$$

NH_2 thus appears as the most abundant *nitrogenated* surface species.

With a view to appreciating how meaningful this conclusion can be on experimental grounds it is in order to compare the different kinds of variation of R_s against P_s according to the assumption which is made concerning the most abundant nitrogenated species. If the latter is identified as NH_3, we could write

$$mP_{NH_3} = \frac{(SNH_3)}{(SH)} = \frac{P_{NH_3}}{K_{NH_3} \cdot (KP_{H_2})^{1/2}} \qquad (7)$$

and m would be proportional to $P_{H_2}^{-1/2}$. If NH were the most abundant nitrogenated species, m would be proportional to $P_{H_2}^{-3/2}$. The resulting variations of R_s in the nearly stoichiometric mixture would be represented in Fig. 2 by curve 3 (NH) or curve 4 (NH_3), whereas curve 1 gives the true variation which is quite different.

It would have been advisable to extend the same analysis to other temperatures in order to know whether NH_2 remains the most abundant nitrogenated species. Unfortunately kinetic experiments are hardly allowed at temperatures higher than 400°C by using the mixture with 17% H_2 because the conditions of equilibrium would be approached too closely. On the other hand, the use of the stoichiometric mixture would result in an inhibition by NH_3 which would be too feeble at temperatures lower than 400°C. What is more easy to monitor at every temperature is the production of NH_3 resulting from the hydrogenation of a prenitrogenated surface. As soon as H_2 contacts such a surface the different equilibria are established and we may look for the most abundant species under these conditions. To this end we have to study the production of NH_3 as a function of time and for various pressures of H_2.

At 301°C, Fig. 7 shows that the equilibrium pressure of NH_3 which is observed at the reactor outlet is proportional to $P_{H_2}^{-1/2}$. Equation (7) suggests that adsorbed NH_3 turns out to be the most abundant species since

$$P_s = K_{NH_3}(KP_{H_2})^{1/2}\frac{(SNH_3)}{(SH)}$$

$$= K_{NH_3}(KP_{H_2})^{1/2}\frac{(SNH_3)}{L-(SNH_3)}$$

and as hydrogen adsorbs immediately on the small fraction of the surface which is not covered with N. If NH_2 were the preponderant species it would result from Eqs. (6) that P_s would be proportional to P_{H_2}. In the latter situation curve 5 of Fig. 7 would be identical with curve 3 initially which is not the case at all.

May we assume the preponderant species during the hydrogenation of preadsorbed N_2 to be the same as that prevailing under the conditions of permanent synthesis? In this respect we can note that the ratios of the surface coverages with the various nitrogenated species depend only on P_{H_2} at a given temperature (and not on θ_N) as has been stated already at the beginning of the present discussion. Molecularly adsorbed NH_3 has been identified to be the most abundant nitrogenated species when preadsorbed N_2 was hydrogenated under P_{H_2} lying between 0.25 and 1 atm. The same must be true when the catalyst is fed with N_2–H_2 reactant mixtures for which the H_2 content varies from 17 to 73% no matter whether the inhibition by NH_3 is undiscernible at this temperature. We cannot state that the same situation would prevail if the H_2 content was lowered to 0.8 or 0.2% as the decrease of P_{H_2} favours the less hydrogenated species to the detriment of the other ones.

4.2. H_2 Coverage of Os Surface

At any temperature the ratio between the rate of N_2 adsorption and the rate of reaction corresponding to the same pressure of N_2 is equal to

$$\frac{r_0}{R_0} = \left[1 + (KP_{H_2})^{1/2}\right]^2 \cong KP_{H_2}. \quad (8)$$

This ratio is easily derived from curves 1 and 5 in Fig. 3 as both these curves correspond to the same N_2 pressure (0.27 atm). The quantity KP_{H_2} is found to vary from 10^4 to 2×10^3 as the temperature increases from 300 to 400°C so that the coverage

$$\theta_H = \frac{(SH)}{L} = \frac{(KP_{H_2})^{1/2}}{1 + (KP_{H_2})^{1/2}}$$

remains very close to 1. This conclusion correlates with the strong H_2 inhibition and the 1 kinetic order with respect to H_2 which have been observed under steady conditions of reaction.

The activation energy of the reaction is derived from curve 1 (35 kcal/mole), whereas that of N_2 adsorption (22 kcal/mole) is given by curve 5. Taking into account Eq. (8) the heat of adsorption of H_2 is found to be equal to 13 kcal/mole. On Ru, the heat of H_2 adsorption determined in the same way was found to be 14 kcal/mole, whereas KP_{H_2} varied correspondingly from 5×10^3 to 10^3. From the latter variation K must be considered as two times smaller on Ru than on Os. There is no inconsistency with the values of the heats of adsorption due to the limited accuracy of their determinations.

Along curves 1 and 2 (Fig. 3) the H_2 inhibition effect is clearly observed and results in an increase of activity when the H_2 pressure is lowered. Nothing so simple can be said when curves 3 and 4 are considered as no increase of activity is brought about by the corresponding decrease of H_2 pressure. As the two curves coincide with one another at low temperatures, it could be inferred that inhibition is no longer exerted upon the catalyst. However, such cannot be the case since the rate of reaction is much less than that of N_2 adsorption. We must therefore conclude that, at low H_2 contents, the H_2 inhibition decreases and allows the NH_3 inhibition to become stronger. If the H_2 inhibition operated only, an increase of activity would be expected from the passage of curve 3 to curve 4. On the other hand, if the catalyst was inhibited by NH_3, an increase of the inhibition would be expected from a lowering of the H_2 pres-

sure due to the shift of the equilibrium of the NH_3 dissociative chemisorption. A compensation effect results so that the highest catalyst activity at low temperature can be observed along the common parts of curves 3 (0.8% H_2) and 4 (0.2% H_2). We have therefore to conclude that in no case can the true activity of Os appear as it remains inhibited either by H_2 or by NH_3. As on Ru, the potential activity of Os is given by the rate of N_2 chemisorption. More than two orders of magnitude separate the potential activity from the best steady one. If reference is made to the stoichiometric mixture, as usually, the gap may reach four orders of magnitude.

4.3. Comparison of Os, Ru, and Fe

In Fig. 3 curves 6 and 6′ represent the Arrhenius plot of the rate of N_2 adsorption (under 0.27 atm) on Ru expressed as the molar amount of N_2 adsorbed per minute and per gram of catalyst (curve 6) and the corresponding turnover frequency in the conversion into NH_3 which would be observed if no inhibition occurred. These data refer to a sample of Ru previously used (*2*) (Johnson & Matthey, Specpure sponge, 30 ppm total impurity) and for which $L = 2.5 \times 10^{-6}$ mole of sites g^{-1}. The difference between the activation energy of N_2 adsorption on Ru and Os (5 kcal/mole) is sufficient to account for the difference between the turnover frequencies.

As N_2 adsorption is faster on Ru than on Os the steady N content is more quickly established on Ru. On the other hand there is no inhibition by NH_3 on Ru which amounts to stating that the corresponding equilibrium constant is high. Both these facts explain that the steady state of activity is reached more rapidly on Ru than on Os, as already stated.

Curve 7 refers to a sample of iron powder (Johnson & Matthey, Specpure sponge, 9 ppm total impurity, 0.1 m^2 g^{-1}) and gives the variation of r_0 as a function of $1/T$ (*13*). In the case of iron $R_0 = r_0$ since there is no H_2 inhibition. R_0 is therefore derived from the variation of R_s against P_s by using Eq. (1). On iron we have shown that the extent of active area depends closely on the reacting conditions (*8*) so that the rate reported here is referred to 1 g as the number of active sites is not known.

Under the steady conditions corresponding to the stoichiometric mixture, Fe is inhibited by NH_3 at a medium level since mP_s lies between 0.1 and 1 when the temperature varies from 300 to 400°C (contact time: 3×10^{-2} sec). Under the same conditions, KP_{H_2} remains higher than 10^3 on Os and Ru and the H_2 inhibition which results on these metals is much more detrimental than the NH_3 inhibition of Fe.

Usually the activities of different catalysts in the NH_3 synthesis are compared with reference to the stoichiometric mixture. In this case the activity of Fe is a little higher than that of Ru (2) but 10^2 times higher than that of Os, so that the decreasing order of activity is

$$\text{Fe} \geq \text{Ru} \gg \text{Os}.$$

This order is right between 300 and 400°C. At temperatures lower that 300°C and down to 200°C, the stoichiometric mixture remains close to the best one on Fe but the activities of Ru and Os can be strengthened by decreasing the H_2 content of the reactant mixture. Os can then be made almost as active as Fe and Ru can reach a level of activity 10 times as high as that of Fe. The decreasing order becomes therefore

$$\text{Ru} > \text{Fe} \geq \text{Os}.$$

If one now takes into account that a good part of the intrinsic activities of these metals is prevented from acting due to inhibition effects, it appears that comparing the rates of N_2 chemisorption on the surfaces of these metals in the absence of any other species should be the most appropriate way of obtaining the most meaningful order of activity. This is so because the chemisorption of N_2 is the slow step of the reaction in every case. From this point of view Ru is

100 times more reactive than Os and Os is from 10 to 100 times more active than Fe, so that we can state that

$$Ru \gg Os \gg Fe.$$

It is worth noting that this order of decreasing activity has been found in the decomposition of NH_3 (*14*) and that the decomposition is inhibited neither by H_2 nor by NH_3.

We shall report later on ways of taking advantage of the high but virtual activity of Os as has been done with Ru (*3*).

REFERENCES

1. Rambeau, G., and Amariglio, H., *J. Chim. Phys.* **75,** 397 (1978).
2. Rambeau, G., and Amariglio, H., *J. Catal.* **72,** 1 (1981).
3. Rambeau, G., and Amariglio, H., *Appl. Catal.* **1,** 291 (1981).
4. Ozaki, A., Aika, K., and Hori, H., *Bull. Chem. Soc. Japan* **44,** 3216 (1971).
5. Dmitrenko, L. M., Ivanova, R. F., and Golubeva, M. A., *Tr. Nauchno Issled. Proektn. Inst. Azotn. Prom. Prod. Org. Sin.* **11,** 102 (1971).
6. Postnikov, V. A., Dmitrenko, L. M., Ivanova, R. F., Dobrolyubova, N. L., Golubeva, M. A., Gapeeya, T. I., Novikoy, Yu. N., Shur, V. B., and Volpin, M. E., *Izv. Akad. Nauk. SSSR Ser. Khim.* **12,** 2642 (1975).
7. Aika, K., Koyama, K., Yamaguchi, J., and Ozaki, A., *Nippon Kagaku Kaishi* **3,** 394 (1976).
8. Amariglio, H., and Rambeau, G., *in* "Proceedings, 6th International Congress on Catalysis, London, 1976" (G. C. Bond, P. B. Wells, and F. C. Tompkins, Eds.), Vol. 2, p. 1113. The Chemical Society, London, 1977.
9. Rambeau, G., and Amariglio, H., *J. Chim. Phys.* **75,** 110 (1978).
10. Ozaki, A., Taylor, H. S., and Boudart, M., *Proc. R. Soc. London Ser. A* **258,** 47 (1960).
11. Aika, K.-I., and Ozaki, A., *J. Catal.* **16,** 97 (1970).
12. Rambeau, G., and Amariglio, H., *J. Chim. Phys.* **75,** 333 (1978).
13. Rambeau, G., and Amariglio, H., to be published.
14. Sokol'skii, D. V., Kuzora, T. V., Kozin, L. F., and Shcherbak, A. I., *Dokl. Akad. Nauk. SSSR* **230,** 620 (1976).